



# Numerical Simulation of Thermal Deformation of Panel Superheater in 600MW Supercritical Circulating Fluidized Bed Boiler

Ye Chen<sup>a,\*</sup>, Nenghong Zheng<sup>b</sup>, Jun Li<sup>c</sup>, Rui Yang<sup>d</sup>

School of Mechanical Engineering, Sichuan University of Science & Engineering, No. 1, Baita Road, Sanjiang New Area, Yibin, Sichuan, China

<sup>a\*</sup>cy32428yr@suse.edu.cn, <sup>b</sup>995873807@qq.com,  
<sup>c</sup>58501323@qq.com, <sup>d</sup>501772641@qq.com

**Abstract.** Targeting the issues of wear, deformation, and tube burst encountered during the operation of the panel superheater in a 600MW supercritical circulating fluidized bed (SCCFB) boiler, this study employs ANSYS finite element analysis software to numerically simulate the temperature distribution and thermal deformation of the panel superheater. A computational model of the panel superheater was established and combined with operational data from the boiler. The results indicate that the maximum wall temperature occurs at the intersection between the panel superheater and the water-cooled wall of the furnace roof, specifically on the fin of pipe No. 50, reaching up to 652.97°C, which exhibits localized overheating. The maximum thermal deviation between the fin and the tube wall is 15.3°C, while the maximum thermal deformation of the tube panel is 215.85 mm. To address the overheating issue, the mass flow rate of the working medium in each tube was adjusted based on the thermal deviation of the tube panel, effectively reducing the peak temperature and mitigating the risk of overheating. This research provides critical insights for further analyzing operational problems of the panel superheater and optimizing its structural design or operating parameters.

**Keywords:** SCCFB boiler; panel superheater; thermal deviation; finite element analysis; thermal deformation

## 1 Introduction

The panel superheater is a critical heating component in supercritical circulating fluidized bed (CFB) boilers. Due to the poor heat transfer capacity of the working medium in the tubes and the uneven distribution of heat load within the furnace, significant thermal deviations often occur between the tubes and panels during prolonged operation. These deviations can lead to localized overtemperatures, resulting in substantial thermal deformation and thermal stress. In severe cases, these conditions can cause pipe

rupture and leakage, which jeopardizes the stable operation of the entire unit. Currently, detection methods primarily involve on-site inspections, including macro and micro analyses, thickness evaluations, chemical composition analysis, metallographic structure analysis, and hardness testing of pipes that have already leaked or ruptured[1-6]. However, these methods are limited in that they typically focus on individual sections of the tube that have failed, which may not accurately represent the overall condition of the tube panel due to the thermal deviations affecting different tubes within the panel. Therefore, to comprehensively and accurately assess the failure of the superheater tube panel under the influence of thermal deviations, it is essential to perform finite element analysis on the superheater to better understand its thermal behavior and failure mechanisms.

This study addresses the failure of the panel superheater due to thermal deviations in a 600 MW SCCFB boiler. A thermal stress analysis model for the panel superheater is developed using ANSYS finite element analysis software, incorporating actual operational parameters of the boiler[7-10]. The model is used to solve and analyze the temperature field distribution and thermal deformation behavior of the tube panel. The results provide valuable insights that can inform the design and operational strategies of SCCFB boilers, contributing to improved performance and reliability.

## 2 Finite Element Calculation Model

### 2.1 Finite Element Model and Computational Boundary Conditions

The panel superheater in a 600 MW SCCFB boiler consists of 55 tubes arranged with a pitch of 60.8 mm and a panel height of 21.7 meters. The tubes are constructed from SA-213 TP347H material, with dimensions of  $\Phi 50.8 \text{ mm} \times 11.5 \text{ mm}$ . The fins are made of 0Cr18Ni9 material, with a flat steel thickness of 6 mm. The operational parameters of the boiler are detailed in Table 1. The finite element model of the panel superheater is illustrated in Figure 1(a). For thermal and structural analyses, 8-node SOLID70 and SOLID185 elements were employed, respectively. Following grid independence verification to ensure a balance between computational efficiency and accuracy, the mesh configuration of the panel superheater model was finalized, as depicted in Figure 1(b). The model comprises approximately 4 million grid elements.

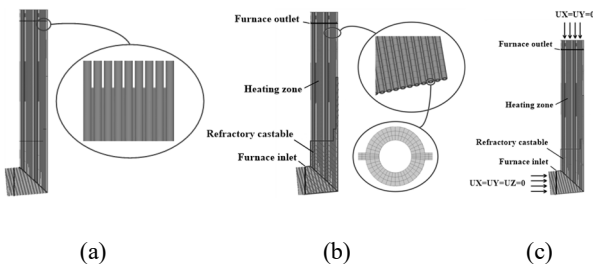


**Fig. 1.** 600 MW SCCFB boiler plate superheater calculation model and boundary conditions.  
 (a, calculation model; b, grid model; c, boundary conditions)

The panel superheater is designed to expand freely within the furnace, and the constraints applied to its computational model should be minimized to ensure calculation accuracy. To achieve this, the structural and force conditions of the tube panel must be analyzed to determine the appropriate mechanical constraints. During operation, the outlet distribution header of the panel superheater is suspended by springs, allowing primarily vertical movement (z-direction) relative to the superheater tube panel. However, at the cross-section where the tubes connect to the outlet header, the tubes remain fixed relative to the superheater tube panel. Therefore, the constraint imposed by the outlet header at the top of the furnace on the tube panel is defined as  $UX = UY = 0$ , with  $UZ$  left unconstrained. The inlet header, on the other hand, exhibits significant stiffness. Additionally, where the superheater tube panel integrates with the water wall, the constraint is considered fully fixed in all directions relative to the water wall to enhance tightness. Thus, the constraint at the inlet is defined as  $UX = UY = UZ = 0$ , while the remainder of the tube panel is allowed to expand freely, as illustrated in Figure 1(c).

**Table 1.** Styles Thermal parameters of real furnace operation of panel superheater.

| Project    | Inlet temperature | Outlet temperature | Flow rate <i>G</i> |
|------------|-------------------|--------------------|--------------------|
| Unit       | °C                | °C                 | t/h                |
| Parameters | 500.8             | 566.3              | 1792.7             |

### 2.2 Equations of Heat Transfer and Elasticity

The research object of this paper is the plate superheater pipe. In order to make the subsequent heat transfer calculation more concise, the steady state thermal conduction differential equation in cylindrical coordinate system is established according to Fourier's law and energy conservation law.

$$\rho c \frac{\partial t}{\partial \tau} = \frac{1}{r} \frac{\partial}{\partial r} (\lambda r \frac{\partial t}{\partial r}) + \frac{1}{r^2} \frac{\partial}{\partial \varphi} (\lambda \frac{\partial t}{\partial \varphi}) + \frac{\partial}{\partial z} (\lambda \frac{\partial t}{\partial z}) \tag{1}$$

$\rho$  is material density, kg/m<sup>3</sup>;  $c$  is Specific Heat Capacity, J/(kg·°C);  $t$  is temperature, °C;  $\tau$  is process time, s;  $\lambda$  is thermal conductivity, W/(m·°C).

From the heat balance of the panel superheater, it can be known that the enthalpy increase of the working medium in the tube per unit time is equal to the heat absorbed from the outside of the furnace, that is:

$$(h_{out} - h_{in}) \cdot G = Q \tag{2}$$

In the aforementioned equation,  $h_{out}$  and  $h_{in}$  denote the specific enthalpy values at the outlet and inlet of the panel superheater, respectively, measured in kJ·kg<sup>-1</sup>·°C<sup>-1</sup>.  $G$  represents the mass flux of the working fluid within the tube, expressed in kg·m<sup>-2</sup>·s<sup>-1</sup>. The total heat absorbed by the tubes,  $Q$ , can be determined using the subsequent equation:

$$Q = \bar{q} \cdot A \tag{3}$$

In the formula,  $A$  denotes the surface area of the heat-absorbing section of the tube, measured in  $m^2$ , and  $\bar{q}$  represents the average heat flux density on the tube surface, in  $kW \cdot m^{-2}$ . The value of  $\bar{q}$  can be determined by integrating the function describing the heat flux density distribution along the height of the furnace, as follows:

$$\bar{q} = \frac{\int_{H_{in}}^{H_{out}} q(H)dH}{H_{out} - H_{in}} \tag{4}$$

Among them,  $H_{out}$  and  $H_{in}$  denote the inlet and outlet heights of the heated section of the tube, in meters  $m$ ;  $q(H)$  represents the heat flux density as a function of height along the furnace [7-8]. By combining equations (2), (3), and (4), the mass flow rate within the tube can be determined using the following equation:

$$G = \frac{l_n \cdot \bar{s} \cdot \int_{H_{in}}^{H_{out}} q(H)dH}{(H_{out} - H_{in})(h_{out} - h_{in})} \tag{5}$$

The local heat flux density at any position along the panel superheater is determined using the thermal deviation across the furnace width, as proposed in reference[9].

That is, the local heat load on the panel superheater tube wall at a distance  $x$  from the furnace water-cooled wall surface is:

$$q_0 = q(H) \cdot Y(x) \tag{6}$$

In the above equation,  $Y(x)$  denotes the thermal deviation coefficient of the tube at a distance  $x$  from the centerline of the furnace water-cooled wall.

Based on the parameters of the working medium inside the panel superheater tubes and the tube dimensions, formula (7) should be used to calculate the heat transfer coefficient of the working medium within the tubes, thereby achieving a better fit with the experimental data[11-14].

$$Nu = 0.00459 Re_w^{0.923} Pr_w^{-0.613} \left( \frac{\rho_w}{\rho_b} \right)^{0.231} \tag{7}$$

In the above equation, the subscript "b" denotes the value at the mainstream steam temperature of the working medium within the tube, while "w" denotes the value at the wall temperature.  $Re$  represents the Reynolds number,  $Pr$  represents the Prandtl number, and  $\rho$  represents the density of the fluid.

$$\begin{aligned}
\varepsilon_x &= \frac{1}{E}[\sigma_x - \mu(\sigma_y + \sigma_z)] + \alpha T, \gamma_{xy} = \frac{1}{G}\tau_{xy} \\
\varepsilon_y &= \frac{1}{E}[\sigma_y - \mu(\sigma_z + \sigma_x)] + \alpha T, \gamma_{yz} = \frac{1}{G}\tau_{yz} \\
\varepsilon_z &= \frac{1}{E}[\sigma_z - \mu(\sigma_x + \sigma_y)] + \alpha T, \gamma_{zx} = \frac{1}{G}\tau_{zx}
\end{aligned} \tag{8}$$

In the formula, E denotes the elastic modulus (GPa);  $\mu$  denotes Poisson's ratio; T denotes temperature ( $^{\circ}\text{C}$ ); G denotes shear modulus (Pa);  $\alpha$  denotes the coefficient of linear expansion.

### 3 Results and Analysis

#### 3.1 Analysis of Temperature Field and Stress Field of Tube Panel

Figure 2 presents a schematic diagram of the temperature field distribution of the tube panel under 100% load conditions. As illustrated, the temperature of each tube closely aligns with that of the working medium inside the tubes due to the low thermal conductivity of the wear-resistant materials in the refractory casting area. As the height of the tube panel increases and extends beyond the wear-resistant layer, the tube wall temperature rises sharply. The maximum temperature occurs at the intersection between the tube panel and the furnace roof water-cooling wall, with a maximum thermal deviation of  $15.3^{\circ}\text{C}$  between the tube and the fin. Along the depth of the furnace, the temperature distribution across the tubes exhibits an initial increase followed by a decrease. This trend is primarily attributed to the fact that tubes No. 47 to No. 55 are covered by a longer wear-resistant layer, resulting in reduced overall heat absorption and a slower temperature rise rate of the working medium within these tubes. Under conditions where the heat transfer efficiency of each tube is not high, the lower temperature of the working medium provides better cooling for the tube panel. However, due to the low mass flow rate within the tubes, the cooling effect is insufficient. Consequently, the maximum temperature of the tube panel is observed at the fin of tube No. 50, reaching  $652.97^{\circ}\text{C}$ , which exceeds the allowable temperature limit of the steel by  $2.97^{\circ}\text{C}$ . Prolonged operation under such overtemperature conditions can lead to overtemperature-induced failures, significantly compromising the boiler's safe operation.

Figure 3 provides a schematic diagram of the thermal stress distribution of the tube panel under 100% load conditions. In conjunction with the temperature field analysis, it is evident that the temperature distribution across the superheater is non-uniform, with significant temperature differences between regions. Temperature variations induce material expansion and contraction, and the mutual constraints between different regions restrict the expansion of high-temperature areas and hinder the contraction of low-temperature areas, resulting in thermal stress. Under the combined influence of these constraints and temperature differences, the maximum thermal stress in the panel superheater occurs at the fin of tube No. 54, reaching 318.9 MPa. This value remains below the tensile strength of the material, which is 520 MPa.

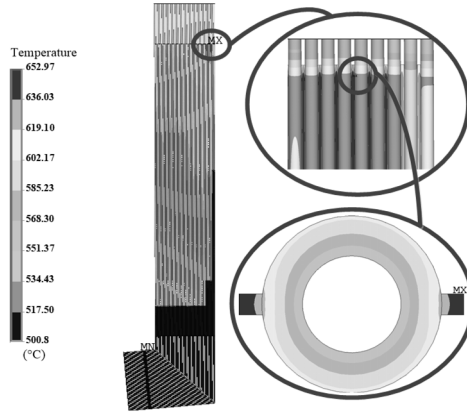


Fig. 2. Temperature calculation results of panel superheater under 100% load condition.

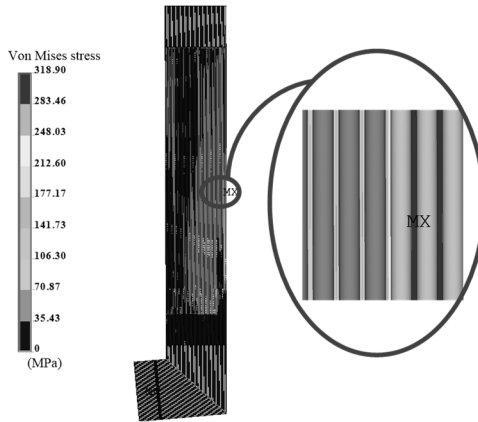


Fig. 3. Thermal stress calculation results of plate superheater under 100% load condition.

### 3.2 Deformation of Tube Panel

Figure 4 illustrates the thermal deformation results of the panel superheater under 100% load conditions. The black border in the figure represents the undeformed tube panel model from the original configuration. The distribution trend of thermal deformation under the three typical operating conditions is consistent. As shown, the maximum deformation of the tube panel occurs at the connection between the top of the panel superheater and the header, with a peak deformation of 215.85 mm. At the inlet area of the tube panel, constraints are applied in the x, y, and z-directions, restricting movement in the x-direction. Despite the presence of thermal deviations in the x-direction, these

constraints limit the displacement of the tube panel, resulting in a relatively small deformation of 51.88 mm in the x-direction. In the y-direction, the tubes of the panel superheater expand freely along the cross-section, with deformations ranging from -0.86 mm to 0.27 mm, indicating minimal deformation.

The mechanical boundary constraints of the panel superheater account for the influence of spring suspension, allowing the tube panel to move freely in the z-direction. The thermal deformation caused by thermal deviations in the x-direction accumulates with increasing tube panel height, leading to a continuous increase in deformation along the furnace height. This deformation reaches its maximum value of 212.33 mm at the furnace outlet. The tube panel exhibits significant bending, which results in uneven erosion of the upper and lower tubes by the furnace materials. This uneven erosion increases the susceptibility of the tube panel to wear, posing a risk to its structural integrity and operational reliability.

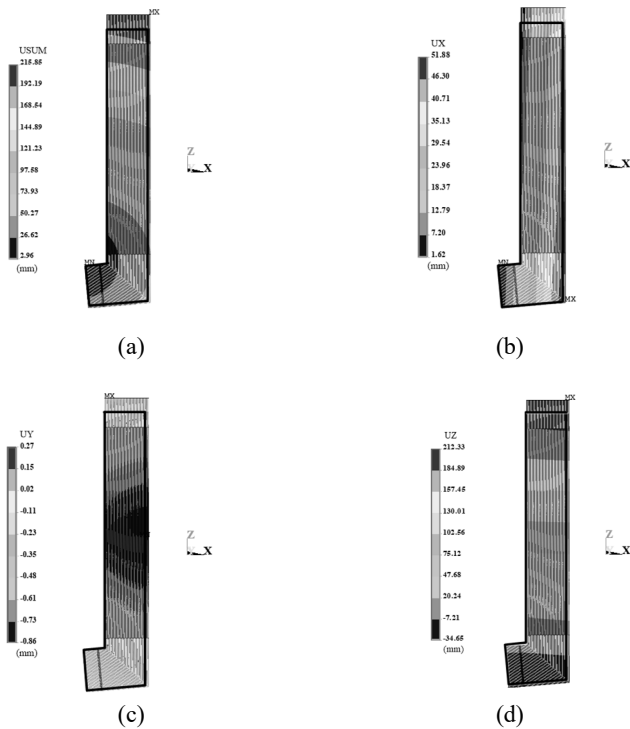


**Fig. 4.** Calculation results of deformation of tube panel under 100% load condition. (a, total deformation of tube panel; b, the x-direction deformation of the tube panel; c, the y-direction deformation of the tube panel; d, the z-direction deformation of the tube panel)

### 4 Improvement Measures

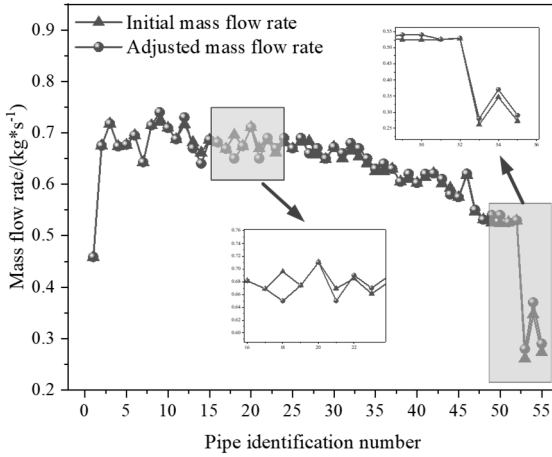


Fig. 5. Mass flow of each tube on the tube panel.

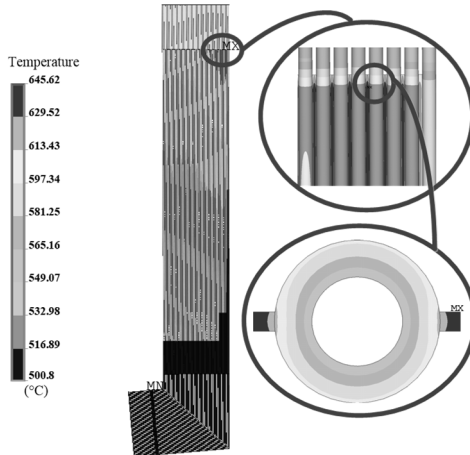


Fig. 6. Temperature field calculation results after mass flow rate adjustment.

Under 100% load conditions, the maximum temperature of tube No. 50 in the panel superheater exceeds the allowable temperature limit of the steel by 2.97°C due to thermal deviation. Prolonged operation under such conditions poses a significant threat to the safe and stable operation of the boiler. To address this issue, the mass flow rate within each tube can be adjusted using throttling devices to reduce the wall temperature. By increasing the mass flow rate in tubes experiencing significant thermal deviation and appropriately adjusting the flow rate in tubes with minor thermal deviation, the outlet steam temperature can be effectively controlled, and the tube wall temperature can be reduced.

Figure 5 compares the mass flow rates in each tube before and after adjustment, while Figure 6 presents the results obtained after recalculating the mass flow rates post-adjustment. As depicted, reducing the flow rate in the central section of the tube panel and increasing the flow rate in the last few tubes significantly lowers the maximum tube wall temperature and reduces the overall thermal deviation of the tube panel. This ensures that the material operates within its allowable temperature range. Compared to the pre-adjustment scenario, the tube wall temperature and thermal stress are reduced, while the thermal deformation of the tube panel shows minimal variation. These adjustments collectively enhance the operational safety and reliability of the unit.

## 5 Conclusions

This study investigates the temperature distribution and thermal deformation of the panel superheater in a 600MW SCCFB boiler under thermal deviation effects, yielding the following key conclusions:

(1) Finite element analysis of the tube panel under 100% load conditions reveals that the maximum wall temperature consistently occurs at the intersection between the panel superheater and the furnace roof water-cooling wall, specifically localized on the fin of tube No. 50. The peak temperature reaches 652.97°C exceeding the allowable temperature limit of the steel by 2.97°C. The maximum thermal stress induced under these conditions is 318.9 MPa, which remains below the material's tensile strength of 520 MPa.

(2) Thermal deformation analysis demonstrates that the maximum displacement of the tube panel under specified boundary conditions is 215.85 mm. The primary contributor to this deformation is unrestricted vertical expansion (z-direction), which accounts for 212.33 mm of the total displacement. Constraints applied in the x-direction at the lower section of the tube panel significantly restrict lateral displacement, limiting x-direction deformation to 51.88 mm despite thermal deviations. In the y-direction, the tube panel exhibits minimal deformation (ranging from -0.86 mm to 0.27 mm) due to free expansion along the cross-sectional normal.

(3) By adjusting the mass flow distribution within the tube panel—specifically reducing flow rates in the central region and increasing flow rates in the rear section—the outlet steam temperature requirements are met while simultaneously reducing the maximum wall temperature and thermal deviation. This optimized flow distribution ensures that the tube panel operates within the allowable temperature range of the steel, thereby enhancing operational safety and structural reliability.

These findings provide critical insights for the design and operational optimization of SCCFB boiler superheaters, addressing thermal management challenges and mitigating risks associated with prolonged overtemperature conditions.

## Acknowledgments

This work was financially supported by the Talent Introduction Project of Sichuan University of Science & Engineering (2019RC18), the Key Laboratory of Process Equipment and Control Engineering in Colleges and Universities of Sichuan Province

(GK201910), and the 2024 Luzhou Science and Technology Program Projects (2024SYF183). Additionally, it was supported by the Scientific Research and Innovation Team Program of Sichuan University of Science & Engineering (SUSE652A004).

## References

1. Adi Himarosa Rela et al. Failure analysis of platen superheater tube, water wall tube, and sealpot plate: A case study from electricity power plant in indonesia[J]. *Engineering Failure Analysis*, 2022, 135.
2. Aliakbar Shami and Seyed Ebrahim Moussavi Torshizi and Ali Jahangiri. Failure Analysis and Remedial Solution Suggestion for Superheater Tubes of a Power Plant Boiler[J]. *Transactions of the Indian Institute of Metals*, 2020, : 1-13.
3. Oh SeBeom et al. Analysis of Platen Superheater Tube Degradation in Thermal Power Plants via Destructive/Non-Destructive Characteristic Evaluation[J]. *Materials*, 2022, 15(2) : 581-581.
4. Chen Y S. Analysis of the Causes and Prevention of Cracking in the Screen Superheater of Circulating Fluidized Bed Boilers [J]. *China Special Equipment Safety*, 2023, 39(02): 66-70. (In Chinese)
5. Zhao P. Analysis of the Causes of Cracking in High-Temperature Superheater Tubes of Supercritical Circulating Fluidized Bed Boilers [J]. *Heat Treatment of Metals*, 2021, 46(06): 225-230. (In Chinese)
6. Meng L Q, Zhang Y L. Failure Analysis of Screen Superheater Tube Burst in Boiler Unit [J]. *Shanxi Metallurgy*, 2023, 46(03): 19-20 + 34. (In Chinese)
7. Chen Ye et al. Experimental Study on the Heat-Transfer Characteristics of a 600 MW Supercritical Circulating Fluidized Bed Boiler[J]. *Energy & Fuels*, 2018, 32(1) : 1-9.
8. Ye Chen et al. An experimental study on the hydrodynamic performance of the water-wall system of a 600 MW supercritical CFB boiler[J]. *Applied Thermal Engineering*, 2018, 141 : 280-287.
9. Niu T T, Zhang W Q, Xin S W, et al. Research on Heat Absorption Deviation Characteristics of Panel superheater in Supercritical Circulating Fluidized Bed Boiler [J]. *Proceedings of the CSEE*, 2022, 42(06): 2227-2238. (In Chinese)
10. Xin S W, Niu T T, Zhang W Q, et al. Research on the Hydrodynamic and Heat Absorption Characteristics of Panel superheater in 600MW Supercritical Circulating Fluidized Bed Boiler [J]. *Journal of Power Engineering*, 2022, 42(08):707-714. (In Chinese)
11. Weiwei Chen et al. An assessment of correlations of forced convection heat transfer to water at supercritical pressure[J]. *Annals of Nuclear Energy*, 2015, 76 : 451-460. <https://doi.org/10.1016/j.anucene.2014.10.027>
12. Swenson H S , Carver J R , Kakarala C R .Heat Transfer to Supercritical Water in Smooth-Bore Tubes[J].*Journal of Heat Transfer*, 1965, 87(4):477.
13. Gupta S, Farah A, King K, et al. Developing new heat-transfer correlation for supercritical-water flow in vertical bare tubes. *Proceedings of the 18th International Conference on Nuclear Engineering (ICONE-18)*, Xi'an, China, 2010, Paper No. 30024.
14. Mokry S, Farah A, King K, et al. Development of a heat-transfer correlation for supercritical water flowing in a vertical bare tube. *Proceedings of the 14th International Heat Transfer Conference (IHTC-14)*, Washington, DC, USA, August 8-13, 2010, Paper No. 22908.

**Open Access** This chapter is licensed under the terms of the Creative Commons Attribution-NonCommercial 4.0 International License (<http://creativecommons.org/licenses/by-nc/4.0/>), which permits any noncommercial use, sharing, adaptation, distribution and reproduction in any medium or format, as long as you give appropriate credit to the original author(s) and the source, provide a link to the Creative Commons license and indicate if changes were made.

The images or other third party material in this chapter are included in the chapter's Creative Commons license, unless indicated otherwise in a credit line to the material. If material is not included in the chapter's Creative Commons license and your intended use is not permitted by statutory regulation or exceeds the permitted use, you will need to obtain permission directly from the copyright holder.

